Determination of the Mott-Hubbard gap in GdTiO_{3}

L. Bjaalie, A. Verma, B. Himmetoglu, A. Janotti, S. Raghavan, V. Protasenko, E. H. Steenbergen, D. Jena, S. Stemmer, and C. G. Van de Walle

Phys. Rev. B **92**, 085111 — Published 6 August 2015

DOI: 10.1103/PhysRevB.92.085111

Determination of the Mott-Hubbard gap in $GdTiO_3$

L. Bjaalie,[1] A. Verma,[2] B. Himmetoglu,[1] A. Janotti,[1] S. Raghavan,[1] V. Protasenko,[2] E. H. Steenbergen,[3] D. Jena,[2] S. Stemmer,[1] and C. G. Van de Walle[1]

[1] *Materials Department, University of California Santa Barbara*
[2] *Department of Electrical Engineering, University of Notre Dame*
[3] *Air Force Research Laboratory, Materials and Manufacturing Directorate, Wright-Patterson AFB, Ohio*

The band gaps of rare-earth titanates are commonly reported to be 0.2-0.7 eV. These values are based on optical reflectivity measurements, from which the onset of optical absorption is derived. Here we report experimental and theoretical results on $GdTiO_3$ (GTO) indicating that the gap is significantly larger. Photoluminescence (PL) measurements show a strong peak near 1.8 eV, consistent with an observed onset in PL excitation (PLE) at about the same energy. First-principles calculations, based either on density functional theory (DFT) with a hybrid functional or on DFT+U, consistently show that the gap is close to 2 eV. We also propose an interpretation of the previously reported optical absorption spectra. Given the similarities in electronic structure between the rare-earth titanates, our results for GTO have repercussions for the other members of the series. The results also affect the design of complex-oxide heterostructures involving these materials.

I. INTRODUCTION

The rare-earth titanates are Mott insulators, in which the energy band gap arises from strong intra-atomic Coulomb electron-electron interactions that split partially filled d or f bands, separating an occupied lower Hubbard band (LHB) from an unoccupied upper Hubbard band (UHB).[1] This Mott-Hubbard gap is fundamentally different from band gaps in conventional semiconductors and insulators, which can be understood in a non-interacting electron picture. In rare-earth titanates such as GTO the Ti atoms assume a Ti^{+3} oxidation state ($3d^1$), with a single unpaired electron per Ti atom. The opening of the gap in these $3d^1$ compounds can be explained within a single-band Hubbard model, in terms of the ratio between the Hubbard U and the d bandwidth.[2] The magnitude of the gap then reflects both the strength of the intra-atomic interactions (U) and the bandwidth.

The value of the Mott-Hubbard gap is not only a key descriptor of Mott insulators, it also determines the functionality of complex oxide heterostructures. Recent experiments have shown the formation of a two-dimensional electron gas (2DEG) at the $SrTiO_3$/GTO interface, with an electron density of 1/2 electron per unit-cell area.[3] The value of the GTO gap determines on which side of the interface these excess electrons reside and the degree of electron confinement, and is therefore an important design parameter.

Previous efforts to determine the Mott-Hubbard gap of GTO were based on optical absorption obtained by Kramers-Kronig analysis of reflectivity data on bulk crystals[4] or thin films grown on $(LaAlO_3)_{0.3}(Sr_2AlTaO_6)_{0.7}$ (LSAT),[5] and from transmission spectroscopy of films grown on $SrLaGaO_4$.[6] These measurements revealed an onset of optical absorption at around 0.7 eV, which was interpreted to correspond to the Mott-Hubbard gap.

Here we present photoluminescence (PL) and PL excitation (PLE) measurements on GTO that produce a strong signal around 1.8 eV. The observation of this PL peak is incompatible with an assumed gap of 0.7 eV, and forces us to reexamine the electronic structure. We therefore perform density functional theory (DFT) calculations using exchange-correlation functionals that are capable of addressing the strong electron-electron interactions that govern the electronic properties of GTO. Conventional exchange-correlation functionals, such as the local density approximation or generalized gradient approximation (GGA), yield an incorrect description of the electronic structure of Mott insulators; they predict GTO to be a metal. These functionals suffer from spurious self-interaction and tend towards excessive delocalization of the electronic density. We therefore use a hybrid functional[7,8] which provides partial cancellation of self-interaction and has been shown to give an accurate description of the electronic and structural properties of a wide range of materials,[9,10] including perovskite Mott insulators.[11] We also use the DFT+U method, which is based on a corrective functional inspired by the Hubbard model, and was designed for the study of Mott insulators.[12] Both approaches produce a Mott-Hubbard gap around 2 eV. This is similar in magnitude to the gaps of the closely related compounds $LaTiO_3$ and $YTiO_3$ when studied with the same methods.[11,13–15] Our conclusion will be that the actual Mott-Hubbard gap of GTO is $\sim$ 2 eV, and we will attribute the absorption onset at 0.7 eV to self-trapped holes.

II. METHODS

Hybrid molecular beam epitaxy was used to grow GTO films .[16] The PL measurements were done by exciting the GTO using a 488-nm ($\hbar\omega$ = 2.54 eV) laser and a 325-nm ($\hbar\omega$ = 3.81 eV) He-Cd laser. For the PLE measurement, PL intensity was measured at a fixed wavelength (760 nm) and the excitation energy was varied from 1.85 eV to 2.35 eV using a continuously tunable super-continuum laser as the excitation source.

For the hybrid functional calculations we adopted the

functional of Heyd, Scuseria, and Ernzerhof[7,8] (HSE), in which a fraction of Hartree-Fock exchange (given by a mixing parameter α=0.25) is mixed with GGA exchange[17] within a range defined by a screening length (0.2 Å^{-1}). The implementation is with projector augmented wave (PAW) potentials in the VASP code.[18,19] For the bulk calculations (20-atom cell), a 500-eV energy cutoff was used for the expansion of plane waves and a $4 \times 4 \times 2$ Γ-centered k-point mesh for the Brillouin-zone integrations. For the self-trapped hole calculations (160-atom supercell), the internal relaxations were performed using a 400-eV energy cutoff and the (1/4, 1/4, 1/4) k-point.

In the DFT+U calculations the corrective functional contains a screened on-site Coulomb repulsion parameter U, which was computed self-consistently using a linear response method,[20] yielding U = 4.38 eV for Gd f orbitals and U = 3.86 eV for Ti d orbitals. Ultra-soft pseudopotentials[21] were employed, as implemented in the Quantum Espresso package.[22] A 60-Ry energy cutoff was used for the expansion of Kohn-Sham states, and a 720-Ry cutoff for the charge-density expansion, using a $6 \times 6 \times 6$ Monkhorst-Pack k-point mesh. For both methods, the Gd f electrons were included in the valence, and all calculations were done using spin polarization.

III. RESULTS AND DISCUSSION

A. Optical measurements

A 20-nm thick GTO film was grown on a cubic LSAT substrate using hybrid molecular beam epitaxy.[16] As a control, both PL and PLE measurements were performed on a bare LSAT substrate without the GTO layer. PL measurements on the bare LSAT substrate show emission from mid-gap states near 1.67 eV (Fig. 1). The GTO-on-LSAT sample displays an additional strong peak at 1.8 eV. A bright red PL signal was also observable with the naked eye at room temperature (inset Fig. 1). No PL peak near 0.7-0.8 eV was observed (see Supplemental Material[23]). From the PLE measurement, a band-edge-like feature close to 1.8 eV can be observed from GTO.

To reconcile a GTO bandgap of 0.7 eV with our 1.8 eV PL observation, one possibility would be to assume that 0.7 eV is the indirect bandgap of GTO while 1.8 eV corresponds to the direct transition. However, given that the LHB and UHB arise from d orbitals that are very localized, band dispersions greater than 1 eV are highly unlikely. Another possibility is that the PL arises not from band-to-band recombination, but from excitonic recombination, defect-to-band transitions, or defect-to-defect transitions.[24] However, all of these recombination mechanisms lead to PL emission either equal to or smaller than the band gap. Therefore, while the PL measurements alone do not allow identifying the precise recombination pathway, the observed PL emission from GTO puts a lower limit on its band gap and indicates this band gap to be greater than or equal to 1.8 eV.

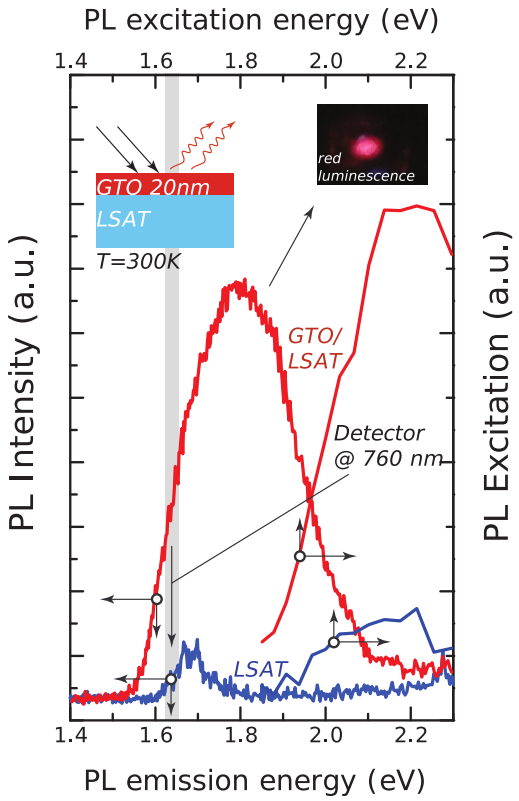

FIG. 1. (Left+Bottom Axes) Room-temperature PL spectrum at 488 nm laser excitation of a 20-nm thin film of $GdTiO_3$ grown on LSAT (red). A peak at 1.8 eV is observed. (Inset) Visually observable red PL from the $GdTiO_3$ sample when pumped with a 325 nm laser. (Right+Top Axes) Room-temperature PLE spectrum (red) of 20-nm thin film of $GdTiO_3$ showing a bandedge like feature near ∼1.8 eV. The pump laser energy was varied, and the detector was tuned to measure the PL intensity at 760 nm. The control measurements of PL and PLE from the bare LSAT substrate are shown in blue.

B. First-principles calculations

Hybrid functional calculations of bulk and optical properties were done using the 20-atom orthorhombic unit cell shown in Fig. 2(a). Both HSE and DFT+U find the ground state to be ferromagnetic, with the Ti $3d^1$ spins aligned, consistent with experiment.[25,26] The occupied f states are located in the low-energy part of the O $2p$ valence bands, and the unoccupied ones in the high-energy part of the Ti $3d$ conduction bands, as can be seen in the density of states (Fig. 3). The main difference between HSE [Fig. 3(a)] and DFT+U [Fig. 3(b)] calculations is the position of the O $2p$ bands, which are located about 2 eV higher in DFT+U. This is expected since DFT+U is not meant to correct the position of these bands.

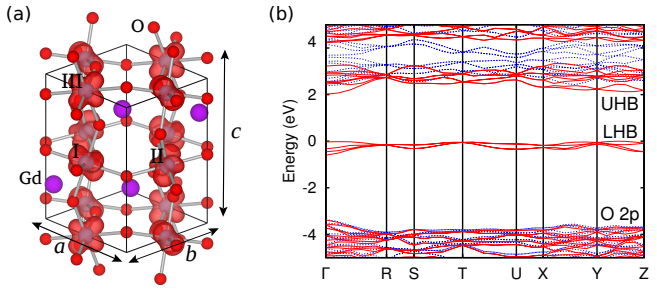

FIG. 2. (a) Ball-and-stick model of the $GdFeO_3$ crystal structure of $GdTiO_3$. The Ti atoms used to define the Ti-O-Ti angles are indicated with I, II, and III. The lower Hubbard band charge density is shown in red (isosurface set to 10% of maximum). (b) Band structure of $GdTiO_3$ calculated using HSE, with red (solid) lines corresponding to spin up states, and blue (dotted) lines to spin down states. The lower Hubbard band is filled, and the upper Hubbard band is empty—the Mott-Hubbard gap occurs between these bands. The zero of energy is set to the highest occupied eigenvalue.

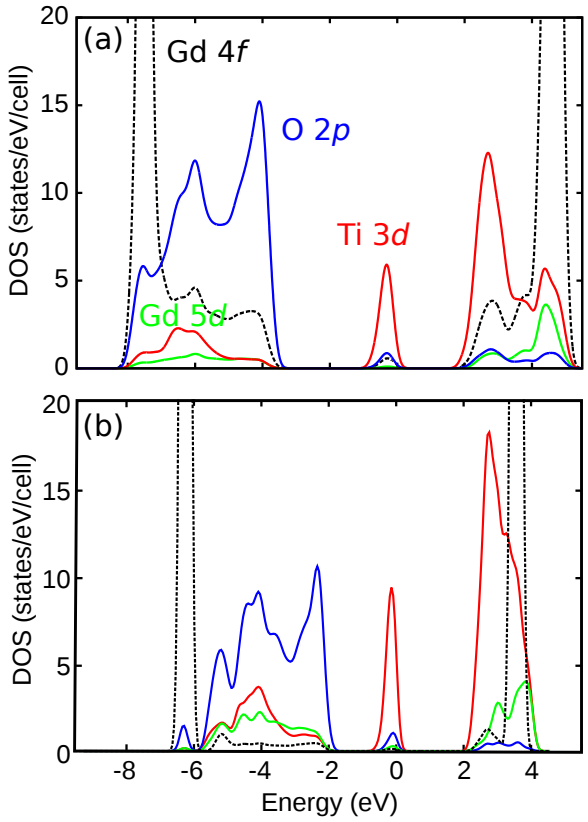

FIG. 3. Atom-projected density of states for $GdTiO_3$ calculated (a) using HSE and (b) using DFT+U. The zero of energy is set to the highest occupied eigenvalue.

Full structural relaxations yield lattice parameters and angles in close agreement with experimental values for bulk GTO, as shown in Table I. The volume is underestimated by 0.7% in HSE, and overestimated by 5.0% in DFT+U, typical for the accuracy provided by these methods.

The band structure from the HSE calculation is shown in Fig. 2(b), giving an indirect band gap of 2.02 eV. The top of the LHB occurs at a point along the Y-Z direction, while the bottom of the UHB occurs at Γ. The direct Γ → Γ band gap occurs at only slightly higher energy, namely 2.05 eV. The dispersion of the individual Hubbard bands is less than 0.7 eV, and the LHB is spin-up, corresponding to ferromagnetic alignment of the Ti $3d^1$ electrons. The LHB charge density is plotted in Fig. 2(a), where orbital ordering of the LHB electrons can be seen. This is a consequence of the large crystal-field splitting of the Ti $3d$ t_{2g} states introduced by the $GdFeO_3$-type distortions, as described in previous work.[14,27] These localized electrons occupy bands derived primarily from d_{xz} and d_{yz} orbitals alternating on every second Ti atom. The band structures from DFT+U calculations (not shown) are very similar, yielding an indirect band gap of 2.21 eV, consistent with a recent study on GTO also using DFT+U.[28] The slight overestimate compared to HSE can be largely attributed to the larger equilibrium volume in DFT+U.

TABLE I. Equilibrium lattice parameters and Ti-O-Ti angles for bulk $GdTiO_3$. Angles referenced to Ti atoms as shown in Fig. 2(a).

	HSE	DFT+U	Exp.[a]
a (Å)	5.351	5.464	5.393
b (Å)	5.725	5.820	5.691
c (Å)	7.627	7.781	7.664
Volume (Å^3)	233.65	247.43	235.22
Ti^I-O-Ti^{II} (°)	144.4	144.1	145.8
Ti^I-O-Ti^{III} (°)	140.4	144.2	144.1

[a] Ref. 29.

Based on this band structure, we expect an onset of direct interband transitions at 2.05 eV. While electric dipole transitions within the d manifold, which gives rise to the LHB and UHB, are forbidden by symmetry, the hybridization with other orbitals, most significantly with O $2p$, leads to finite optical transition elements. The effect of hybridization of Ti d states with O p, Gd d and Gd f states is clearly visible in the atom-projected density of states shown in Fig. 3. The presence of strong optical transitions is confirmed by our first-principles calculations of the absorption coefficient, defined by

$$\alpha_i(\omega) = \frac{\sqrt{2}\omega}{c}\sqrt{|\epsilon_{ii}| - \mathrm{Re}(\epsilon_{ii}(\omega))}, \qquad (1)$$

where $\epsilon_{ii'}$ is the dielectric tensor and ω the frequency. The dielectric tensor was computed with the HSE functional within the PAW formalism as described in Ref. 30. A 0.2 eV Gaussian smearing of the band occupancies was

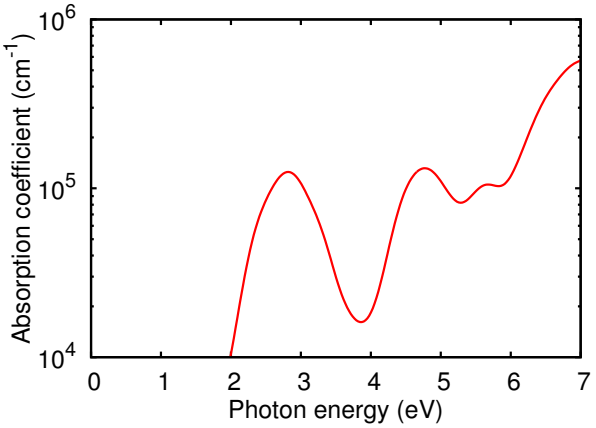

FIG. 4. Total optical absorption for bulk $GdTiO_3$, calculated with HSE and averaged over the x, y, and z directions.

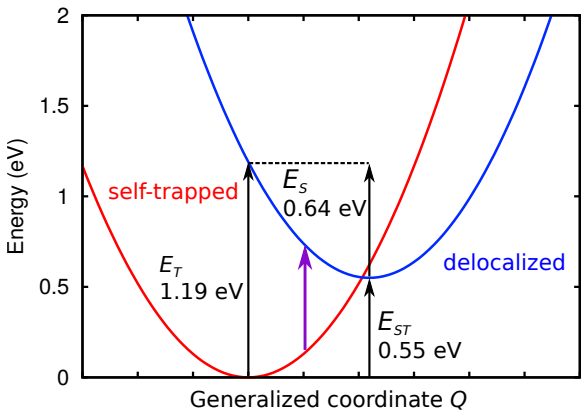

FIG. 5. Configuration coordinate diagram for a self-trapped and delocalized hole in $GdTiO_3$. E_{ST} is the net energy gain from self-trapping, E_S is the lattice energy cost, and E_T is the vertical transition energy. The purple arrow indicates the possiblity of excitations below E_T due to vibrational broadening.

used, leading to a broadening of the absorption coefficient. The results shown in Fig. 4 indicate strong optical transitions starting around 2.0 eV, with a peak at 2.8 eV. Recombination will occur at lower energies, closer to the band edge, since electrons excited to higher energies in the UHB will lower their energy nonradiatively before recombining with holes.

C. Discussion

Both PL/PLE measurements and first-principles calculations are therefore consistent with a Mott-Hubbard gap of around 2 eV in GTO. This raises the question of the origin of absorption with an onset around 0.7 eV observed in reflectivity measurements.[4–6] We attribute this onset to transitions between self-trapped holes and the LHB.[15] The presence of self-trapped holes in rare-earth titanates has been inferred from thermally activated p-type hopping conductivity.[31] Recent transport measurements on Sr-doped GTO also show that holes readily localize in the material.[32] Optical excitations of electrons from the LHB to the self-trapped hole state can then occur.

Using a 160-atom supercell (a $2 \times 2 \times 2$ enlargement of the 20-atom unit cell) we investigate the behavior of a single missing electron, simulating both localization (self-trapped hole) and delocalization (equal hole density on all Ti atoms). The results are shown in Fig. 5. Self-trapping indeed occurs, and the self-trapped configuration is more stable than the delocalized state by 0.55 eV, the self-trapping energy E_{ST}. A lattice- energy cost of 0.64 eV E_S is associated with the self-trapping of the hole; this value is found from the energy difference between the atomic structures of the self-trapped and delocalized hole configurations, calculated in a charge-neutral supercell. The transition energy E_T is the sum of the lattice-energy cost (0.64 eV) and the self-trapping energy (0.55 eV); the resulting value of 1.19 eV corresponds to a peak in the absorption spectrum. The *onset* of absorption can occur at significantly lower energies due to vibrational broadening (as indicated by the purple arrow in Fig. 5). We propose that such transitions involving self-trapped holes are responsible for the low-energy onset in the optical absorption spectra of GTO.

The possibility of luminescence resulting from self-trapped holes should also be examined. There are two conceivable mechanisms that could be probed using PL/PLE. First, excitation of an electron from the LHB to the self-trapped hole state could occur, but after this excitation the small-polaron state is gone—all that remains is a local distortion of the crystal structure, which will decay via phonon emission. Second, an electron excited to the UHB could recombine with a small-hole-polaron state. A transition at this energy is actually more likely to be nonradiative,[33] and indeed, PL measurements around 0.7 eV do not show any signal in this energy range.[23]

IV. CONCLUSIONS

In summary, we have presented results of optical measurements and first-principles calculations indicating that the Mott-Hubbard gap of GTO is significantly larger than the previously accepted value of 0.7 eV. The calculations predict a gap of 2.0 eV, in good agreement with the observed 1.8 eV PL peak, which constitutes a lower limit to the band gap. Our results for GTO indicate that the accepted values of the Mott-Hubbard gap of other rare-earth titanates may also need to be revised. Establishing the correct values of these gaps will enable a better understanding of the electron-electron interactions in $3d$ transition-metal compounds. Correct gap values are also essential for accurate design of heterojunctions based on

rare-earth titanates.

ACKNOWLEDGMENTS

The authors would like to thank A. Alkauskas for useful discussions. This work was supported by the MURI program of the Office of Naval Research, Grant Number N00014-12-1-0976 and by the NSF MRSEC program (DMR-1121053). Computational resources were provided by the Center for Scientific Computing at the CNSI and MRL (an NSF MRSEC, DMR-1121053) (NSF CNS-0960316), and by the Extreme Science and Engineering Discovery Environment (XSEDE), supported by NSF (OCI-1053575 and DMR07-0072N).

[1] N. F. Mott, Proc. Phys. Soc. London Sect. A **62**, 416 (1949).
[2] A. Fujimori et al., Phys. Rev. Lett. **69**, 1796 (1992).
[3] P. Moetakef et al., Appl. Phys. Lett. **99**, 232116 (2011).
[4] D. A. Crandles, T. Timusk, J. D. Garrett, and J. E. Greedan, Physica C **201**, 407 (1992).
[5] P. Moetakef, D. G. Ouellette, J. Y. Zhang, T. A. Cain, S. J. Allen, and S. Stemmer, J. Cryst. Growth **355**, 166 (2012).
[6] M. N. Grisola, F. Y. Bruno, D. Sando, H. J. Zhao, E. Jacquet, X. M. Chen, L. Bellaiche, A. Barthélémy, and M. Bibes, Appl. Phys. Lett. **105**, 172402 (2014).
[7] J. Heyd, G. E. Scuseria, and M. Ernzerhof, J. Chem. Phys. **118**, 8207 (2003).
[8] J. Heyd and G. E. Scuseria, J. Chem. Phys. **121**, 1187 (2004).
[9] J. Paier, M. Marsman, K. Hummer, G. Kresse, I. C. Gerber, and J. G. Angyán, J. Chem. Phys. **124**, 154709 (2006).
[10] P. Rivero, I. P. R. Moreira, G. E. Scuseria, and F. Illas, Phys. Rev. B **79**, 245129 (2009).
[11] J. He and C. Franchini, Phys. Rev. B **86**, 235117 (2012).
[12] V. I. Anisimov, F. Aryasetiawan, and A. I. Lichtenstein, Phys. Condens. Matter **9**, 767 (1997).
[13] F. Iori, M. Gatti, and A. Rubio, Phys. Rev. B **85**, 115129 (2012).
[14] F. El-Mellouhi, E. N. Brothers, M. J. Lucero, I. W. Bulik, and G. E. Scuseria, Phys. Rev. B **87**, 035107 (2013).
[15] B. Himmetoglu, A. Janotti, L. Bjaalie, and C. G. Van de Walle, Phys. Rev. B **90**, 161102 (2014).
[16] P. Moetakef, J. Y. Zhang, S. Raghavan, A. P. Kajdos, and S. Stemmer, J. Vac. Sci. Technol. A **31**, 041503 (2013).
[17] J. P. Perdew, K. Burke, and M. Ernzerhof, Phys. Rev. Lett. **77**, 3865 (1996).
[18] G. Kresse and D. Joubert, Phys. Rev. B **59**, 1758 (1999).
[19] G. Kresse and J. Furthmüller, J. Comput. Mater. Sci. **6**, 15 (1996).
[20] M. Cococcioni and S. de Gironcoli, Phys. Rev. B **71**, 035105 (2005).
[21] D. Vanderbilt, Phys. Rev. B **41**, 7892 (1990).
[22] P. Giannozzi, S. Baroni, N. Bonini, M. Calandra, R. Car, C. Cavazzoni, D. Ceresoli, C. L. Chiarotti, M. Cococcioni, I. Dabo et al., J. Phys. Condens. Matter **21**, 395502 (2009).
[23] See Supplemental Material.
[24] P. Y. Yu and M. Cardona, *Fundamentals of Semiconductors*, (Springer, New York, 2010), 4th ed.
[25] Carl W. Turner and E. Greedan, J. Solid State Chem. **34**, 207 (1980).
[26] A. C. Komarek, H. Roth, M. Cwik, W.-D. Stein, J. Baier, M. Kriener, F. Bourée, T. Lorenz, and M. Braden, Phys. Rev. B **75**, 224402 (2007).
[27] E. Pavarini, A. Yamasaki, J. Nuss, and O. K. Andersen, New J. Physics **7**, 188 (2005).
[28] L.-J. Yang, Y.-K. Weng, H.-M. Zhang, and S. Dong, J. Phys. Condens. Matter **26**, 476001 (2014).
[29] D. A. Maclean, H.-N. Ng, and J. E. Greedan, J. Solid State Chem. **30**, 35 (1979).
[30] M. Gajdos, K. Hummer, G. Kresse, J. Furthmüller and F. Bechstedt, Phys. Rev. B **73**, 045112 (2006).
[31] H. D. Zhou and J. B. Goodenough, J. Phys.: Condens. Matter **17**, 7395 (2005).
[32] D. G. Ouellette, P. Moetakef, T. A. Cain, J. Y. Zhang, S. Stemmer, D. Emin, S. J. Allen, Sci. Rep. **3**, 3284 (2013).
[33] A. Alkauskas, Q. Yan, and C. G. Van de Walle, Phys. Rev. B **90**, 075202 (2014).